

Indonesian Journal of Computing, Engineering, and Design

Journal homepage: http://ojs.sampoernauniversity.ac.id/index.php/IJOCED

Lessons Learned from Challenges in Developing a Test Setup to Replace a Faulty Universal Testing Machine

Jen Hua Ling^{1*}, Wei Jun Chin¹, Bing Liang Ling¹, Vincent Liang Cheng Su¹

¹ Centre for Research of Innovation & Sustainable Development, School of Engineering and Technology, University of Technology Sarawak, 96000 Sibu, Sarawak, Malaysia

*Corresponding email: lingjenhua@uts.edu.my

ABSTRACT

This study addresses the challenges encountered in developing a test setup to replace a malfunctioning Universal Testing Machine (UTM). The setup was designed using a portal frame, hydraulic jack system, data acquisition system, and beam reaction system to simulate compressive forces on concrete-filled tube (CFT) specimens. Significant issues arose, including deformation of the steel plate, which failed to uniformly distribute stress; excessive out-of-plane deformation of the supporting steel beam; and load cell damage due to overloading. These problems resulted from inappropriate load simulation, inaccurate measurements, and safety concerns. Despite multiple mitigation attempts, the setup was ultimately unsuccessful and discontinued. Displacement discrepancies reached 90.9% and 76.7% in Setup 1 and Setup 2, respectively, while strength discrepancies of 31.9% to 46.2% were observed in identical specimens. This research highlights the complexities of replicating precise testing conditions and underscores the need for thorough planning and expertise in experimental design. To guide future setups, this study recommends a strength hierarchy, in ascending order: specimen, hydraulic cylinder, load cell, steel beam, and portal frame, to ensure safety and reliability in test execution.

ARTICLE INFO

Article History:
Received 01 Jan 2025
Revised 26 Jun 2025
Accepted 10 Oct 2025
Available online 21 Oct 2025

Keywords:

Hydraulic cylinder, Load cell, Portal frame, Test setup, Universal testing machine.

1. INTRODUCTION

The universal testing machine (UTM) is one of the most widely used tools in structural engineering research, primarily for conducting tensile and compression tests (Topón-Visarrea et al., 2020). It plays a vital role in accurately assessing the mechanical properties of materials (Chenthil et al., 2022), such as tensile and compressive strength, yield strength, elasticity, and ductility. By loading specimens to failure, researchers gain insights into material behaviour structural performance under stress.

unexpected equipment However, malfunctions can severely disrupt testing and compromise research outcomes. This study initially aimed to determine the compressive strength of concrete-filled tube (CFT) specimens using a UTM. Unfortunately, the machine failed before testing began. Due to time constraints, an alternative setup was developed, comprising a portal frame, hydraulic jack, steel beam, and data acquisition system, to replicate typical UTM loading conditions and measurement capabilities.

Despite careful planning, the alternative setup encountered several issues that rendered the results unreliable. Repeated troubleshooting attempts

introduced further complications, ultimately leading to the termination of testing to avoid equipment damage. With no reliable data obtained, the study shifted focus to reviewing the challenges and failures faced during the development of the non-standard testing setup.

While many studies have investigated the mechanical behavior of CFT specimens using UTMs (Yii and Ling, 2024; Mollakhalili et al., 2024; Miao et al., 2024; Lu et al., 2024; Woldemariam et al., 2020; Abduljabar Abdulla, 2021), none appear to address the challenges that arise when such equipment is unavailable. Most published work assumes the use of fully functional UTMs and offers limited guidance for researchers working under equipment constraints.

Some studies have focused on upgrading or customizing UTMs. For instance, Huňady et al. (2024) digitized an analogue UTM to enable fatigue testing. Topón-Visarrea et al. (2020) developed a control system to test textile fibers and sponges. Huerta et al. (2010) designed and validated a custom UTM for thin films. Mathew and Francis (2019) design and build a UTM capable of handling up to 10 kN loads for polymer materials. However, these studies still depend on operational UTMs and do not explore solutions when a UTM is non-functional.

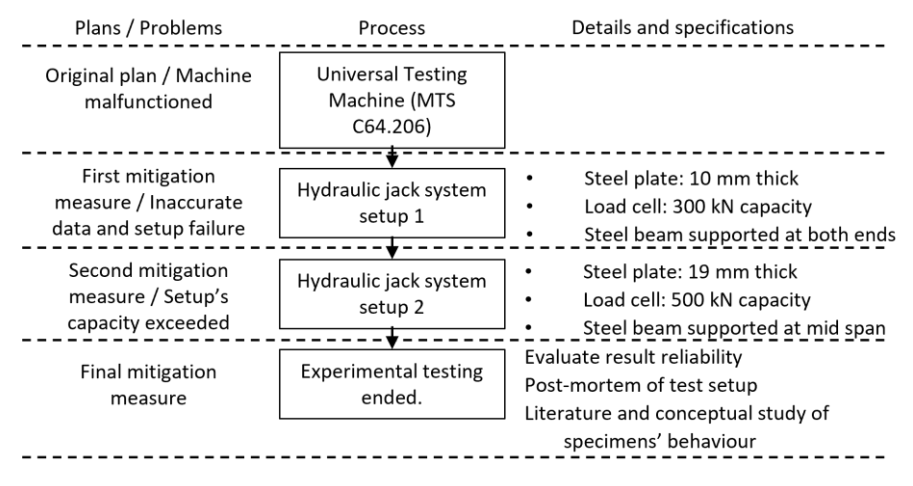


Figure 1. Overview of the test programme

This paper addresses that gap by documenting an attempt to replicate UTM functionality using available resources, highlighting both the technical difficulties and lessons learned. The aim is to provide useful insights for researchers facing similar challenges and to encourage more transparent reporting of experimental setbacks structural in engineering research. The scientific contribution lies in offering a structured evaluation of the challenges in developing an alternative loading system, including problems related load distribution. measurement accuracy, and system stability. These insights are rarely reported but are valuable for researchers operating under equipment limitations.

This paper outlines the initial testing plan, the development implementation of the alternative setup, the causes of failure encountered, and the key lessons learned. By documenting this experience, it contributes to the broader body of knowledge in structural engineering experimentation. It also provides guidance and cautionary insights for future studies involving non-standard methods, emphasizing importance of careful planning, rigorous validation, and adaptability in research design.

2. METHOD

Figure 1 presents the overview of the test programme, showing the plan changes and problems encountered. Setup details are also provided.

2.1. Initial Plan

The original plan involved testing concrete-filled tube (CFT) specimens under compression using a universal testing machine (UTM). The UTM available at the heavy structure laboratory of the University of Technology Sarawak, Malaysia, was a Brand *MTS* model C64.206

with a load capacity of 2000 kN (Figure 2 and Table 1).



Figure 2. Static Hydraulic Universal Testing Machine (Brand: *MTS*, Model: C64.206)

Table 1. Specifications of MTS C64.206

UTM Specifications	Details
Rated force capacity	2000 kN
Test spaces	Dual
Actuator Stroke	250 mm
Actuator speed	0.5 – 85 mm/min
Crosshead speed	250 mm/min
Column spacing (Test	720 mm
space width)	
Maximum tension space	920 mm
Maximum compression	1000 mm
space	
Diameter of round	15 – 70 mm
specimens	
Thickness of flat	10 – 70 mm
specimens	
Compression Platen	240 x 240 mm
(Square)	

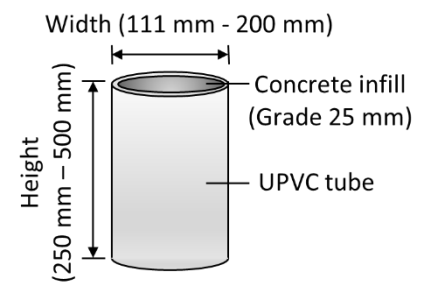


Figure 3. Concrete-filled tube (CFT) specimens

The CFT specimens were cylindrical, with diameters ranging from 111 mm to 200 mm and heights between 250 mm and 500 mm (**Figure 3**). These sizes were well within the UTM's 1000 mm height and 720 mm width compression test space, making

the UTM compatible for testing (**Table 2**). Additionally, the UTM's 240 mm x 240 mm compression platen provided sufficient coverage to ensure uniform application of the compression force, as it adequately covered the specimens' diameters, which did not exceed 200 mm.

Table 2. Compatible check of UTM against the specimen sizes

UTM Specifications (MTS Model C64.206)	CFT specimen sizes	Compatibility check
Maximum compression space: 1000 mm	Height: 250 mm to 500 mm	Specimens fit within the 1000 mm space
Compression Platen (Square): 240 x 240 mm	Diameter: 111 mm to 200 mm	The entire specimen cross-sectional area is covered by the platen
Column spacing (Test space width): 720 mm	Diameter: 111 mm to 200 mm	Sufficient space around specimens for easy handling

2.2. Alternative Testing Setup

Due to a UTM malfunction, an alternative testing setup was developed to replicate the usual loading conditions and measurement accuracy. This setup included a portal frame, a steel beam system, and a scaffold (Figure 4). Each component was independently anchored to the strong floor. The portal frame held the hydraulic cylinder, transferring its force to the strong floor, while the steel beam supported the specimen, providing the necessary reaction force (Figure 5). To prevent deformations of the portal frame and steel beam from affecting the accuracy of displacement measurements, scaffold holding the LVDTs was kept separate. Any disturbance to the scaffold

would compromise the accuracy of the measurements.

A hydraulic jack system, comprising of a hydraulic cylinder and a hydraulic hand pump from Brand Energac, was employed to apply load to the specimens. The hydraulic cylinder, model RR10018, had a maximum operating pressure of 700 bar and a loading capacity of 933 kN (Table 3). Its 460 mm stroke was sufficient to accommodate the elastic shortening of the specimens under compression, with specimen heights ranging from 250 mm to 500 mm. The hydraulic hand pump, model P464, was used because (a) it had a maximum operating pressure of 700 bar, matching that of the hydraulic cylinder, and (b) its reservoir capacity of 7423 cm³ exceeded the oil capacity required by the hydraulic cylinder, which was 6132 cm³ (Table 4).

Table 3. Hydraulic cylinder (Brand: *Enerpec,* Model: RR10018)

Hydraulic cylinder	Details
Specifications	
Maximum Operating	700
Pressure (bar)	
Capacity Class (tonnage)	100
Maximum Cylinder	933
Capacity Advance (kN)	
Stroke (mm)	460
Collapsed Height A (mm)	687
Extended Height B (mm)	1147
Return Type	Double-Acting,
	Hydraulic Return
Cylinder Effective Area	133.3
Advance (cm²)	
Cylinder Effective Area	62.2
Retract (cm²)	
Oil Capacity Advance (cm ³)	6132
Oil Capacity Retract (cm ³)	2861
Weight (kg)	117

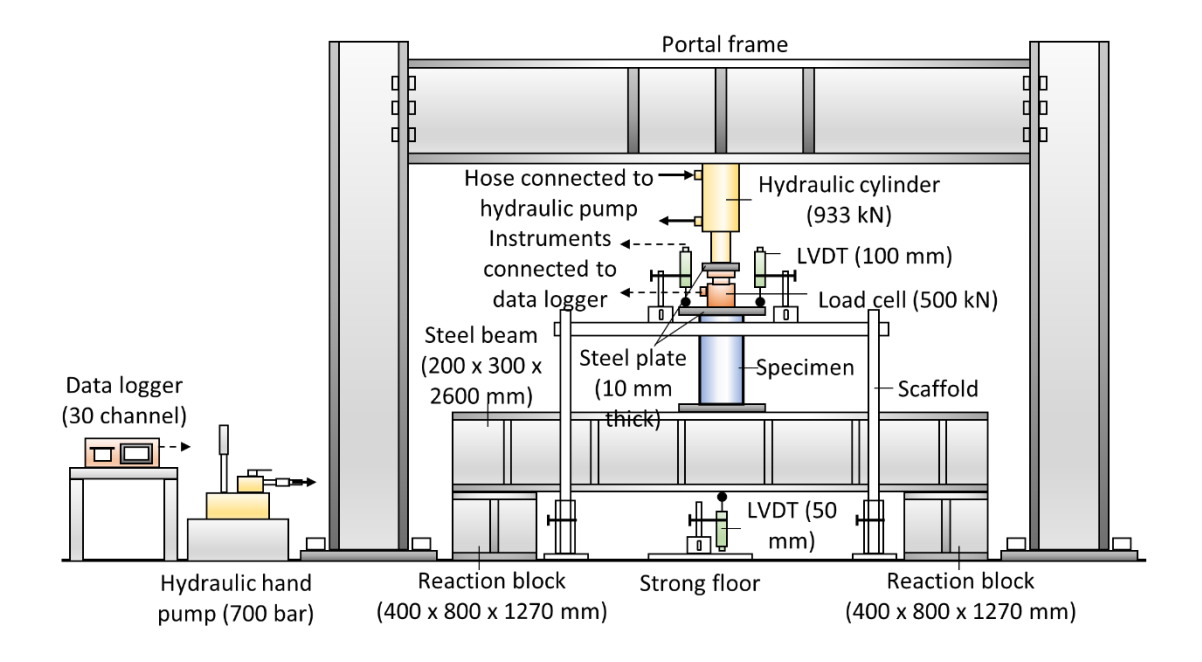


Figure 4. Schematic drawing of test Setup 1

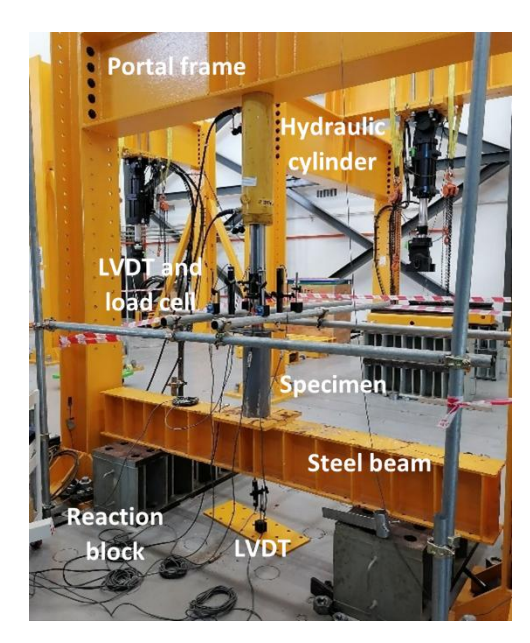


Figure 5. Test Setup 1

The data acquisition system consisted of a data logger, a load cell, and five linear variable differential transformers (LVDTs) (**Table 5**). The data logger had 30 built-in channels, which was sufficient for logging the six measuring instruments (i.e., one load cell and five LVDTs). A 300 kN load cell was placed between the hydraulic cylinder and the specimen to measure the load acting on the specimen. A 250 mm x 250 mm x 10 mm mild steel plate was placed

between the load cell and the specimen to disperse the stress, ensuring the specimen was uniformly loaded during testing.

Table 4. Hydraulic hand pump (Brand: *Enerpec,* Model: P464)

Hydraulic hand pump Specifications	Details
Maximum Operating Pressure (bar)	700
Pressure Rating 1st Stage (bar)	14
Pressure Rating 2nd Stage (bar)	700
Cylinder Compatability	Double-
	acting
Pump Type	Two Speed
Reservoir Capacity (cm³)	7423
Usable Oil Capacity (cm³)	7423
Maximum Flow at Rated	4.75
Pressure	cm³/stroke
Oil Displacement Per Stroke 1st Stage (cm³)	126.20
Oil Displacement Per Stroke 2nd Stage (cm³)	4.75
Maximum Handle Effort (kg)	49
Piston Stroke (mm)	38.1
Valve Operation	Manual
Power Source	Manual
Weight (kg)	27.7

Instruments	Brand / Model	Specifications	Speed / Accuracy	Units
Data logger	TML / TDS530-30	30 channels	0.1s measurement speed	1
Load Cell	TML / CLJ-300KNB	Capacity 300 kN	± 0.1 kN	1
	TML / CLJ-500KNB*	Capacity 500 kN	± 0.1 kN	1
Linear variable differential	TML / CDP-50	50 mm stroke	± 0.01 mm	1
transformers (LVDT)	TML / CDP-100	100 mm stroke	+ 0.01 mm	Δ

Table 5. Specification of data acquisition instruments used

^{*}use after CLJ-300KNB was damaged.

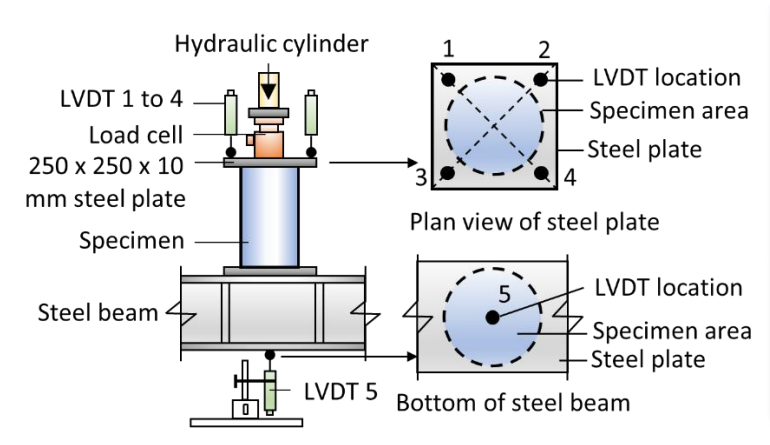




Figure 6. Locations of LVDTs

Four LVDTs (100 mm stroke), mounted to the scaffold using magnetic stands, were positioned at each corner of the steel plate, intersecting at the specimen's centroid (Figure 6). The average vertical displacement measured by these LVDTs represented the vertical displacement of the top surface of the specimen, Δ_{top} . One LVDT (50 mm stroke) was placed below the steel beam along the specimen's centroid axis to measure the deflection of the steel beam during testing, Δ_{bot} . The elastic shortening of the specimen, Δ , under compression, was determined subtracting Δ_{bot} from Δ_{top} (Equation 1).

$$\Delta = \Delta_{top} - \Delta_{bot} = \frac{\Sigma \Delta_{1-4}}{4} - \Delta_5 \tag{1}$$

where Δ_{1-4} are the vertical displacements measured by LVDTs 1 to 4 (mm), and Δ_5 is the vertical displacement measured by LVDT 5 (mm).

This calculation is based on the following assumptions:

- The steel plate remained flat and did not undergo any elastic shortening throughout the test.
- The steel beam did not experience lateral torsional buckling, where the deflection led only to vertical displacement, not horizontal displacement.
- The cross-section of the steel beam remained unchanged, without distortion or elastic shortening after deflection.
- The specimen did not experience outof-plane deformation.

Before testing, the specimen's height, diameter, and weight were measured to ensure consistency in dimensions and density, confirming uniform workmanship in sample preparation. All measuring instruments connected to the data logger were initialized to zero. A vertical load was then applied to the specimens through the hydraulic cylinder, with readings taken at every 5 kN load increment. The test continued until the load peaked and then reduced by 20% from its peak.

2.3. Modified Test Setup

The test setup encountered unforeseen issues during testing. The initial assumptions were inaccurate. The steel plate between the load cell and the specimen exhibited significant curvature, with its centre sinking into the specimen and its corners uplifting by approximately 7.34 mm (Figure 7).

This response invalidated the test, impairing accurate measurement of the specimen's displacement for several reasons:

 The curvature induced non-uniform stress distribution on the specimen, concentrating high stress at its centroid

- and deviating from the intended load condition.
- LVDTs 1 to 4 yielded inconsistent readings, with discrepancies ranging from 24.2% to 90.9%, which were substantial (Table 6).

In addition, the steel beam supporting the specimen experienced deflection due to its large clear span (**Table 7**). This posed a risk of lateral torsional buckling, which can lead to out-of-plane deformation constituting both vertical and lateral displacements. Excessive out-of-plane deformation can cause dislocation of the specimen, affecting the accuracy of displacement measurements, as the LVDTs were set to measure only the vertical displacement.

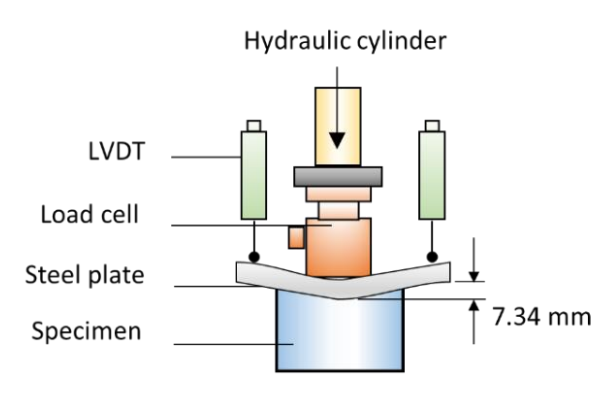




Figure 7. Failure of steel plate

Table 6. Inconsistent LVDT reading due to failure of the steel plate

Specimen		Displacement (mm)		Maximum	Minimum	Discrepancy,	
	LVDT 1	LVDT 2	LVDT 3	LVDT 4	value, ∆ _{max}	value, ∆ _{min}	D (%)
					(mm)	(mm)	
S3D1	4.55	5.15	2.58	3.5	5.15	2.58	49.9
I3D1	5.11	4.19	7.24	5.4	7.24	4.19	42.1
IS3D1	3.87	4	5.07	5.55	5.55	3.87	30.3
S3D2	3.62	3.88	7.37	6.48	7.37	3.62	50.9
13D2	4.36	4.61	3.76	4.96	4.96	3.76	24.2
IS3D2	8.55	6.43	8.48	6.68	8.55	6.43	24.8
T500-120	4.7	5.84	3.72	4.4	5.84	3.72	36.3
C500-120	2.71	3.39	3.7	4.26	4.26	2.71	36.4
C500-80	5.32	7.12	4.61	4.21	7.12	4.21	40.9
C500-114 T1	7.35	4.39	4.18	0.67	7.35	0.67	90.9
C500-114 T2	6.04	4.83	4.41	2.95	6.04	2.95	51.2
C500-114 T3	5.38	6.17	5.95	7.16	7.16	5.38	24.9
S500-114 T1	7.14	9.65	4.11	5.11	9.65	4.11	57.4
S500-150 T1	7.88	6.17	4.72	4.22	7.88	4.22	46.4

^{*}The data was obtained from the tests done using test setup 1. Discrepancy, $D=\frac{\Delta_{max}-\Delta_{min}}{\Delta_{max}}$

Table 7. Deflection of the steel beam under ultimate load

Specimen	Load (kN)	Displacement measured by LVDT 5 (mm)
S3D1 T1	162.2	2.13
I3D1	148.1	2.05
IS3D1 T1	165.7	1.92
S3D2 T1	300.0	3.36
I3D2 T1	332.9	3.53
IS3D2	297.9	3.17
T500-120	404.7	3.75
C500-120	380.4	3.82
C500-80	400.1	4.59
C500-114 T1	195.9	2.86
C500-114 T2	172.1	1.87
C500-114 T3	183.3	2.33
S500-114 T1	218.6	2.68
S500-150 T1	357.1	3.98

To address these issues, the test setup was modified as follows: (Figure 8 and Figure 9)

- The existing steel plate was replaced with a thicker one (250 mm x 250 mm x 19 mm) for greater rigidity.
- The reaction blocks were moved to the centre of the steel beam to eliminate its deflection.
- LVDT 5 was removed as no deflection of the steel beam was expected from the new setup.

With these modifications, the elastic shortening of the specimen under compression was calculated based on the average value of LVDTs 1 to 4 (Equation 2):

$$\Delta = \frac{\Sigma \Delta_i}{4} \tag{2}$$

where Δ_i is the vertical displacement measured by LDVTs 1 to 4 (mm).

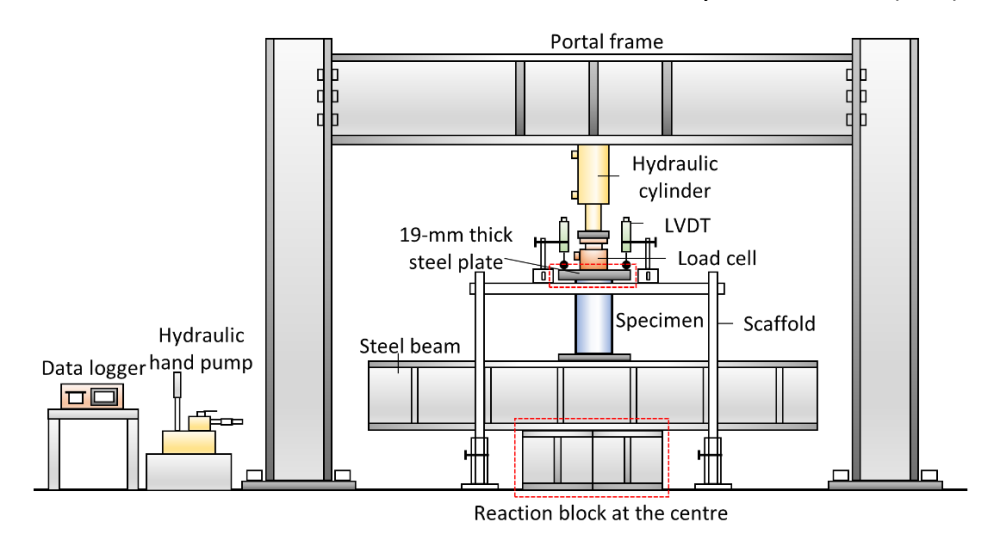


Figure 8. Modifications made on the test setup



- (a) Reaction blocks moved to the center
- (b) Plate's thickness increased to 19 mm

Figure 9. Mitigation measure for the test setup

This calculation was based on the following assumptions:

- The steel plate remained flat throughout the test.
- The steel plate, steel beam, and reaction block did not undergo elastic shortening.
- The specimen, steel beam and reaction blocks did not experience out-of-plane deformation.

2.4. Experiment Terminated

Despite efforts to mitigate the problems with the test setup, additional complications arose (**Figure 10**):

- The load cell's capacity (300 kN) was exceeded, causing damage and rendering the measurement of the specimen's load capacity inaccurate.
- Out-of-plane deformation of the steel beam occurred due to instability under excessive load, again proving the assumptions were incorrect.

 This deformation caused the specimen to tilt, resulting in inaccurate vertical displacement measurements.

Even with the use of a thicker steel plate, discrepancies in the LVDT readings persisted. This issue stemmed from the out-of-plane deformation of the steel beam, not from the curving of the steel plate. The discrepancies ranged from 3.8% to 76.7% (**Table 8**). Although this was an improvement over the previous setup, it was still significant enough to invalidate the test results.

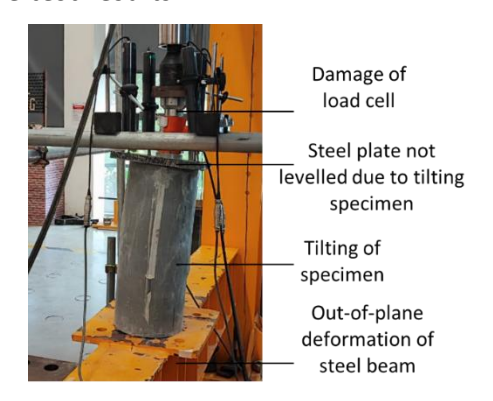


Figure 10. Instability and failure of the test setup

Table 8. Discrepancy of LVDT readings of test setup 2

Specimen	Load		Displacen	nent (mm)		Maximum	Minimum	Discrepancy,
	(kN)	LVDT 1	LVDT 2	LVDT 3	LVDT 4	value,	value, ∆ _{min}	D (%)
						Δ _{max} (mm)	(mm)	
S3D1 T2	93.8	8.92	8.41	8.65	8.21	8.92	8.21	8.0
IS3D1 T2	96.4	12.2	10.15	11.08	9.16	12.2	9.16	24.9
IS3D1 T3	82.0	7.72	5.78	8.81	7.13	8.81	5.78	34.4
S3D2 T2	204.7	3.36	3.56	2.09	1.94	3.56	1.94	45.5
S3D2 T3	160.2	7.99	7.69	7.99	7.77	7.99	7.69	3.8
13D2 T2	176.3	16.44	13.08	8.92	7.5	16.44	7.5	54.4
13D2 T3	202.3	12.79	11.01	10.18	8.71	12.79	8.71	31.9
C500-40	871.1	3.13	7.06	8.54	13.41	13.41	3.13	76.7
S500-114 T2	102.8	7.58	7.62	7.3	7.32	7.62	7.3	4.2
S500-114 T3	145.1	4.36	4.11	4.39	4.03	4.39	4.03	8.2
C500-150 T1	235.6	5.29	4.2	4.68	4.53	5.29	4.2	20.6
C500-150 T2	240.6	10.02	9.34	10.79	10.4	10.79	9.34	13.4
S500-150 T2	244.0	10.85	12.36	7.64	9.92	12.36	7.64	38.2
S500-150 T3	242.2	10.4	10.42	10.8	11.37	11.37	10.4	8.5
S500-200	426.7	3.27	4.46	9.69	12.69	12.69	3.27	74.2
C500-200 T1	315.3	16.57	16.9	13.78	14.61	16.9	13.78	18.5

These issues persisted even after replacing the 300 kN load cell with a larger capacity model (TML CLJ-500KNB, 500 kN). Consequently, the experiment was terminated to prevent further damage to the test setup and instruments. Continuing the experiment was deemed pointless as the results were already inaccurate and unreliable, and the defective specimens could not be re-tested. The presented data are from tested specimens; the remaining specimens were untested and disposed of.

3. RESULTS AND DISCUSSIONS

The setup issues were identified in three main areas: inappropriate load simulation, inaccurate measurements, and safety concerns.

3.1. Inappropriate Load Simulation

The hydraulic cylinder applied force to the specimen, which was measured by an 80 mm diameter load cell. The specimen's diameter ranged from 111 mm to 200 mm. To distribute stress evenly, a 10 mm thick steel plate was placed between the load cell and the specimen. However, this plate was not rigid enough, causing depression in the centre and lifting at the corners, resulting in uneven stress distribution on the specimen's concave top surface (Figure 11). This uneven stress risked inaccurately

simulating loading conditions and measuring the specimen's true load-bearing capacity.

The loading condition significantly affected the load-bearing capacity of the CFT specimens. Identical specimens such as S3D1, IS3D1, S3D2, I3D2, S500-114, and S500-150 showed varying results under different test setups (**Table 9**). Test setup 1, using a 10 mm thick steel plate, consistently demonstrated higher strength compared to setup 2, which used a 20 mm thick steel plate. Strength discrepancies ranged from 31.9% to 46.2%.

The steel plate's thickness influenced the specimen loading. A thicker plate distributed stress more uniformly due to its rigidity (Figure 12). The thin plate primarily loaded the concrete, while the thick plate represented loading both the concrete and the tube. Table 9 indicates that specimens tested with the thin plate (setup 1) generally had higher strength than those tested with the thick plate (setup 2), consistent with literature findings. The greatest concrete confinement occurs when only the concrete is loaded, with the tube providing circumferential restraint (O'Shea and Bridge, 2000).

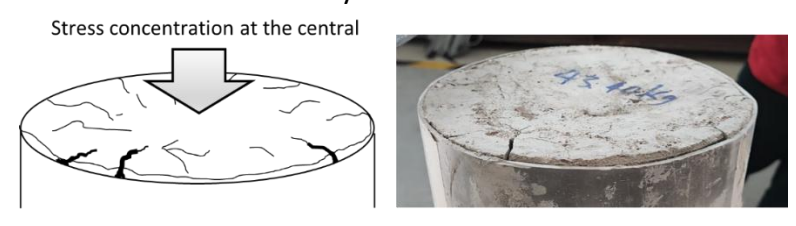


Figure 11. Concave top surface of the specimen after testing

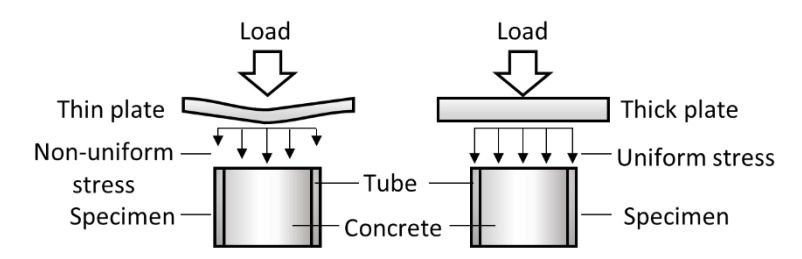


Figure 12. Effects of the plate thickness on the loading conditions on CFT specimens

Table 9. Ultimate strength of CFT specimens

Specimen	No	Ultimate	Discrepancy,	
	=	Test setup 1, P _{u,1}	Test setup 2, P _{u,2}	D (%)*
S3D1	T1	162.2		42.2
	T2		93.8	
I3D1		148.1		N/A
IS3D1	T1	165.7		46.2
	T2		96.4	
	T3		82.0	
S3D2	T1	300		39.2
	T2		204.7	
	T3		160.2	
13D2	T1	332.9		43.1
	T2		176.3	
	T3		202.3	
IS3D2		297.9		N/A
T500-120		404.7		N/A
C500-120		380.4		N/A
C500-80		400.1		N/A
C500-40			871.1	N/A
C500-114	T1	195.9		N/A
	T2	172.1		
	T3	183.3		
S500-114	T1	218.6		43.3
	T2		102.8	
	T3		145.1	
C500-150	T1		235.6	N/A
	T2		240.6	
S500-150	T1	357.1		31.9
	T2		244.0	
	T3		242.2	
S500-200			426.7	N/A
C500-200	T1		315.3	N/A

^{*}Discrepancy, $D = \frac{P_{u.1} - P_{u.2}}{P_{u.1}}$, where $P_{u,1}$ is the ultimate load from test setup 1, and $P_{u,2}$ is the average ultimate load from test setup 2.

N/A = Not applicable, as only one specimen was tested, and discrepancy requires at least two specimens.

3.2. Inaccurate Measurements

Unlike the UTM, which simultaneously induces load, measures load, and measures displacement, the test setup had several limitations. In this setup, the hydraulic cylinder, load cell, and LVDTs performed these functions separately. Ideally, all instruments should align along

the specimen's centroid to ensure accurate measurements. However, only the load cell and hydraulic cylinder could be positioned along this axis, requiring a different placement for the LVDTs.

To address this, four LVDTs were placed at the corners of a steel plate intersecting at the specimen's centroid

(**Figure 6**). This arrangement ensured that their average displacement measurement represented the centroid's displacement, assuming the steel plate remained undeformed. However, in practice, the steel plate experienced significant deformation (**Figure 7**), leading to inaccurate measurements.

An LVDT was placed underneath the steel beam to monitor its deflection (Figure 4). This deflection was subtracted from the vertical displacement measured by the four LVDTs to determine the specimen's elastic shortening under load (Equation 1). This calculation was valid if (a) only the specimen deformed and (b) the steel beam deflected vertically only. However, the steel plate and beam between the two sets of LVDTs were also susceptible to elastic shortening under axial load. Additionally, the steel beam's deflection might include out-of-plane displacement, resulting in horizontal movement that was not measured during the test.

In test setup 2, reaction blocks were placed directly beneath the specimen to eliminate mid-span deflection (Figure 8). The specimen's elastic shortening was determined using the four LVDTs on the steel plate (Equation 2), assuming no deformation in the elements underneath the specimen (i.e., the steel beam and reaction blocks). However, both the steel beam and reaction blocks could still experience elastic shortening, affecting the LVDT measurements. Additionally, the steel beam exhibited out-of-plane deformation as it reached its lateral torsional buckling limit (Figure 10), further compromising the accuracy of the specimen's elastic shortening measurements.

3.3. Safety Concerns

Based on the manufacturer's specifications, the load cells CLJ-300KNB

and CLJ-500KNB had capacities of 300 kN and 500 kN, respectively. However, they were unsuitable for the test due to the following reasons:

- The hydraulic cylinder, Enerpac RR10018, could induce loads up to 933 kN.
- Some specimens could withstand greater loads, as they had not yet failed during testing.

Due to negligence, load cell CLJ-300KNB was once loaded up to 871.1 kN (**Table 9**, specimen C500-40), far exceeding its 300 kN capacity. Consequently, its top mounting tilted, indicating its damage (**Figure 13**).

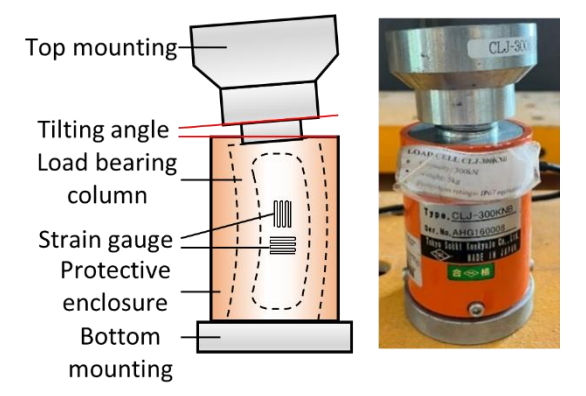


Figure 13. Damage of load cell

A load cell is a transducer that converts mechanical force into an electrical signal via strain gauges bonded to its load-bearing column (Figure 13). When a load is applied, the column deforms, altering the strain gauges' resistance and thus changing the voltage signal. A data logger then converts this signal into a readable force measurement.

The tilt of the load cell's top mounting was a symptom of yielding, indicating permanent deformation. This inelastic deformation means the load cell no longer follows Hooke's law, leading to inaccurate measurements. To prevent the risk of excessive forces damaging the load cell, the hydraulic cylinder's capacity should not exceed the load cell's capacity. In

destructive tests, the specimen's load capacity should not surpass the capacities of both the load cell and the hydraulic cylinder to ensure accurate results.

The capacities of the load cell and hydraulic cylinder can be obtained from manufacturer specifications, while the specimen's load capacity can be estimated through calculations. For instance, a 200 mm diameter concrete cylinder with a strength of 25 N/mm² would have a capacity of at least 785.4 kN. Literature suggests that concrete-filled tube (CFT) specimens may be stronger. The tube confines the concrete, thereby enhancing the concrete's compressive strength (Guo et al., 2024). Simultaneously, the concrete resists the tube's inward buckling, subsequently enhancing its axial strength (Alatshan et al., 2020). This synergistic renders greater compressive strength than the combination of the two components (Han et al., 2014).

The entire test setup must be considered as an integrated system, where the weakest component dictates performance. In this case, the portal frame and the steel beam were critical load reaction systems. Excessive deflection and out-of-plane deformation of the steel beam indicated that the reaction system had reached its limits, affecting accuracy and posing safety risks.

A test setup should not fail before the specimen. A specimen's load capacity may be estimated, but it is difficult to predict accurately. It is often determined through experimental tests. Although safety factors may be incorporated into the design of a test setup, there is still a risk of underdesigning it. To protect the system, a hydraulic cylinder with a lower capacity than the portal frame, load cell, and steel beam may be used. This prevents them from the risk of overloading due to negligence.

In practice, the portal frame and steel beam are standard structural elements used repeatedly over various specimens and test setups. They must meet stringent performance criteria to prevent excessive deformation. Excessive portal frame deformation may dislocate the hydraulic cylinder, causing deviation in the direction of force imposed on the specimen. Similarly, excessive steel beam deformation can dislocate the specimen. resulting in inaccurate displacement measurements. Both scenarios complicate experiment and jeopardize the credibility of the test results.

Often, even if the load capacities are not exceeded, a load reaction system (e.g., portal frame and steel beam) is deemed unsuitable for the test when its deflection exceeds certain limits. For instance, at the University of Technology Sarawak, during testing and commissioning, a portal frame exceeding 3 mm deflection in the x-, y-, and z-directions was considered compliance (University of Technology Sarawak, 2017). Adopting this principle in testing, an additional LVDT could be placed on the portal frame to monitor its deflection during testing. If deflection exceeds 3 mm, the portal frame should be strengthened. This measure ensures structural integrity, as well as maintains the accuracy and credibility of test results.

For infinite repeated use without compromising performance, a structural element should not exceed its fatigue or endurance limit. Below this limit, the stress level is insufficient to cause crack propagation, thus preventing damage (Hajshirmohammadi and Khonsari, 2021). According to Boardma (1990), the fatigue limit of steel is approximately half its ultimate strength. Exceeding this limit may compromise the element's lifespan and structural integrity. The ultimate load capacity of steel sections can be calculated using Eurocode 3 (British Standards, 2010).

These considerations establish a clear hierarchy of strength within the test setup (Figure 14). The test setup must not fail before the specimen. The hydraulic cylinder acts as a safeguard, limiting applied loads to protect critical components, ensuring accurate results and preserving the setup for future use.

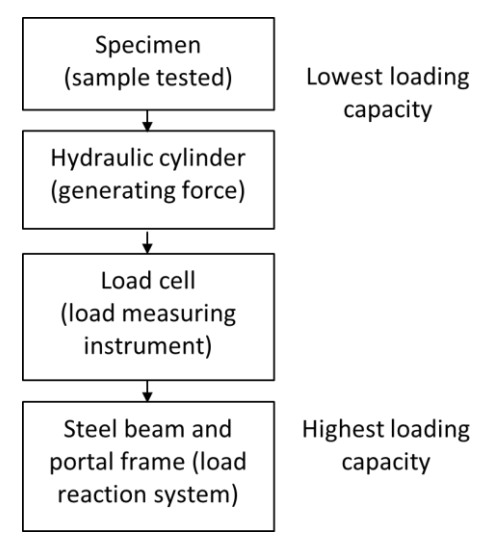


Figure 14. Hierarchy of strength of the test setup

4. CONCLUSION

This paper documents the challenges in developing a test setup to replace a malfunctioning Universal Testing Machine (UTM), aiming to replicate its loading conditions and measurement accuracy. Despite several modifications, the setup remained unreliable, with displacement discrepancies reaching 90.9% and 76.7% in Setup 1 and Setup 2, respectively. Strength discrepancies of 31.9% to 46.2% were also observed in identical specimens. As a result, the test was discontinued.

The study reveals that such test setups may fail due to (a) inappropriate load simulation, (b) inaccurate measurements, and (c) safety risks. These challenges underscore the complexities involved in non-standard testing arrangements in structural engineering research.

A key lesson from this work is the importance of the "hierarchy of strength," which should follow an ascending order: specimen, hydraulic cylinder, load cell, steel beam, and portal frame. This hierarchy ensures that the specimen fails before any other component, helping to minimize equipment damage and maintain safety.

While this case study provides useful insights, it is based on a single empirical attempt and may not cover all potential failure modes. Even when known pitfalls are avoided, alternative test setups may still encounter unforeseen issues. As such, this study does not aim to definitively propose a universal alternative to the UTM.

For future studies, it is advisable to begin with preliminary trials using dummy specimens and proceed to specimens only after confirming the setup's reliability. It is also important to estimate the load capacity of components, including the specimen, measuring instruments, portal frame, and support system, while adhering to the hierarchy of strength. These practices can improve both safety and reliability, leading to better outcomes in structural testing.

REFERENCES

Abduljabar Abdulla, N. (2021). Strength models for uPVC-confined concrete. *Construction and Building Materials*, 310, 125070. https://doi.org/10.1016/j.conbuildmat.2021.125070

Alatshan, F., Osman, S. A., Mashiri, F. & Hamid, R. (2020). Explicit simulation of circular CFST stub columns with external steel confinement under axial compression. *Materials*, 13(1), 23. https://doi.org/10.3390/ma13010023

- Boardma, B. (1990). Fatigue resistance of steels: ASM handbook, Volume 1: Properties and selection: Irons, steels, and high-performance alloys. ASM Handbook Committee. https://doi.org/10.31399/asm.hb.v01.9781627081610
- British Standards. (2010). Eurocode 3: Design of steel structures Part 1-1: General rules and rules for buildings, MS EN 1993-1-1:2010.
- Chenthil, M. E., Sai Praneeth, S., Shalom Anand, D. & Srikanth, M. (2022). Universal Testing Machine. *International Journal of Innovative Research in Technology*, 9, 1572 -1575.
- Guo, J., Wang, Y., Deng, Z. & Chang, P. (2024). Research on the axial compression performance of coral concrete-filled aluminum alloy tube columns. *Case Studies in Construction Materials*, 20, e02952. https://doi.org/10.1016/j.cscm.2024.e02952
- Hajshirmohammadi, B. & Khonsari, M. M. (2021). An approach for fatigue life prediction based on external heating. *International Journal of Mechanical Sciences*, 204, 106510. https://doi.org/10.1016/j.ijmecsci.2021.106510
- Han, L. H., Li, W. & Bjorhovde, R. (2014). Developments and advanced applications of concrete-filled steel tubular (CFST) structures: Members. *Journal of Constructional Steel Research*, 100, 211-228. https://doi.org/10.1016/j.jcsr.2014.04.016
- Huerta, E., Corona, J. E. & Oliva, A. I. (2010). Universal testing machine for mechanical properties of thin materials. *Revista Mexicana De F'Isica*, 56, 317–322.
- Huňady, R., Sivák, P., Delyová, I., Bocko, J., Vavro, J. & Hroncová, D. (2024). Upgrade of the universal testing machine for the possibilities of fatigue tests in a limited mode. *Applied Sciences*, 14, 3973. https://doi.org/10.3390/app14103973
- Lu, S., Yang, J., Wang, J. & Wang, L. (2024). Experimental and theoretical analysis of steel tubed geopolymer concrete columns under axial compression. *Construction and Building Materials*, 411, 134277. https://doi.org/10.1016/j.conbuildmat.2023.134277
- Mathew, S. J. & Francis, V. (2019). Development, validation and implementation of universal testing machine. Master thesis, *Jönköping University*.
- Miao, W., Ye, Y., Lei, R. H. & Jiang, H. (2024). Performance of seawater sea sand concrete-filled bimetallic tube (SSCFBT) stub columns under axial partial compression. *Structures*, 60, 105812. https://doi.org/10.1016/j.istruc.2023.105812
- Mollakhalili, A., Tabatabaeian, M. & Khaloo, A. (2024). Experimental and numerical investigations on the post-heating performance of concrete-filled pultruded GFRP tubes under concentric compression. *Composite Structures*, 331, 117914. https://doi.org/10.1016/j.istruc.2023.105812
- O'shea, M. D. & Bridge, R. Q. (2000). Design of circular thin-walled concrete filled steel tubes. *Journal of Structural Engineering*, 126, 1295-1303. https://doi.org/10.1061/(ASCE)0733-9445(2000)126:11(1295)
- Topón-Visarrea, L., Zapata, M. & Vallejo Mancero, B. Automation of a Universal Testing Machine for Measuring Mechanical Properties in Textile Fibers. In: Botto-Tobar, M., León-Acurio, J., Díaz Cadena, A. & Montiel Díaz, P., eds. Advances in Emerging Trends and Technologies, 2020// 2020 Cham. Springer International Publishing, 189-199

- University of Technology Sarawak, 2017. Specification and schedule: Nominated sub-contract for design, supply, install, testing and commisioning heavy structure laboratory for civil engineering, School of Engineering and Technology, University of Technology Sarawak, Malaysia.
- Woldemariam, A. M., Oyawa, W. O. & Nyomboi, T. (2020). Experimental studies on the behavior of concrete-filled uPVC tubular columns under axial compression loads. *Cogent Engineering*, 7, 1768649. https://doi.org/10.1080/23311916.2020.1768649
- Yii, P. Z. F. & Ling, J. H. (2024). Behaviour of concrete-filled plastic tube (CFPT) embedded with reinforcement bar under axial compressive load. *Borneo Journal of Sciences and Technology*, 6, 28-38. http://doi.org/10.35370/bjost.2024.6.1-04